Investigations on OTC-MPPT Strategy and FRT Capability for PMSG Wind System with the Support of Optimized Wind Side Controller Based on GWO Technique

Mohamed Metwally Mahmoud[1,*], Basiony Shehata Atia[2], Mohamed Khalid Ratib[1], Mohamed M. Aly[3], Abdallah E. Elwakeel[4], Abdel-Moamen M. Abdel-Rahim[1]

[1] Department of Electrical Engineering, Faculty of Energy Engineering, Aswan University, Egypt.
[2] Field Service Engineer at Rapiscan Service Center Egypt, American Science and Engineering, Inc. Cairo, Egypt.
[3] Department of Electrical Engineering, Faculty of Engineering, Aswan University, Egypt.
[4] Department of Agricultural Engineering, Faculty of Agriculture and Natural Resources, Aswan University, Egypt.

Abstract **— Stable operation of permanent-magnet synchronous generator-based wind turbines (PMSG-WTs) is a challenging and complicated objective. Dealing with the hard situations and complex operations of the PMSG-WTs has recently become a hot issue in modern power systems. The abilities of PMSG-WT to ride over faults and operate at maximum power point (MPP) are the most critical requirements for national grid regulations. To maintain the system's reliability, PMSG-WT should remain linked to the grid during normal and abnormal conditions. Furthermore, PMSG-WT has the potential to inject reactive power during failures. It produces active and reactive power to maintain grid voltage immediately after the fault is cleared. This research uses MATLAB/Simulink to investigate the operation at MPP during wind speed changes and FRT capability during three-phase fault of PMSG-WT to validate the support of grey wolf optimizer (GWO)-based PI controllers at the wind side converter. The findings reveal that, when PMSG-WT is exposed to a fault, active and reactive power react in a complementary manner, i.e., active power to the grid drops, and injected reactive power rises to stabilize the system. While during wind speed changes the system achieves MPP operation using an optimal torque control strategy, and the output power follows the wind variations.**

[*] Corresponding author.
E-mail: metwally_m@aswu.edu.eg

http://dx.doi.org/10.38028/esr.2021.04.0007
Received November 21, 2021. Revised December 11, 2021. Accepted December 23, 2021. Available online January 25, 2021.

Index Terms: **Grid code compliance, grey wolf optimizer (GWO), grid fault, MPP, PMSG-WT.**

List of abbreviations

ANNs – artificial neural networks
APA – affine projection algorithm
CSA – cuckoo search algorithm
FACTS – flexible alternating current transmission system
FLC – fuzzy logic controller
FRT – fault ride-through
GSA – gravitational search algorithm
GSC – grid-side converter
GWO – grey wolf optimizer
GCC – grid code compliance
OTC – optimal torque control
PI – proportional-integral
MSC – machine-side converter
MPPT – maximum power point tracking
PSO – particle swarm optimizer
PMSG – permanent magnet synchronous generator
WOA – whale optimizer algorithm
WT – wind turbine
WECS – wind energy conversion system
BCS – braking chopper system
BA – bee algorithm
ESA – energy storage apparatuses
WSC – wind side converter

I. Introduction

In today's electricity system, renewable energies play a critical role, with wind energy having the quickest implementation in many nations [1, 2]. Wind energy is less expensive than other renewable energy sources, delivers electricity with less environmental impact, and is more reliable [3]. The global capacity of installed wind power from 2001 to 2022 is presented in [4]. Several nations have created operational guidelines for the integration of

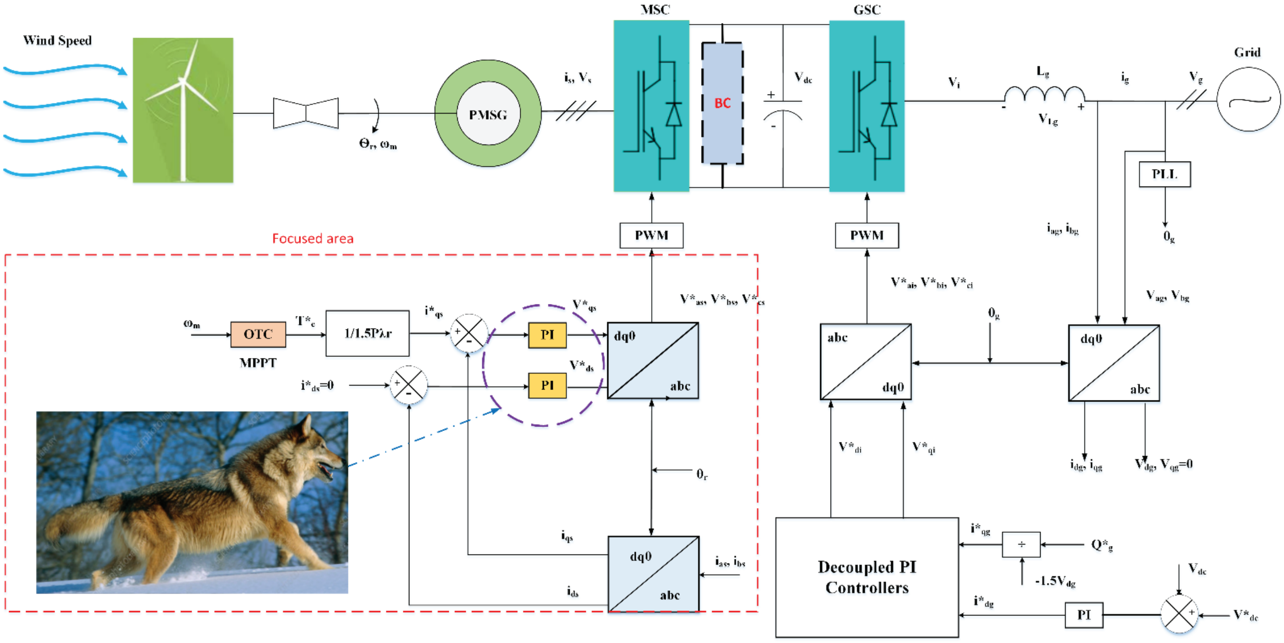

Fig. 1. The addressed system.

dispersed power based on grid codes. Due to their unique characteristics, such as variable speed and real-time power management, permanent-magnet synchronous generators (PMSGs) are the most extensively utilized wind energy conversion devices [5, 6].

During typical operating conditions, both the grid side and wind side power converters are used to manage DC link voltage, actual power transfer, and reactive power transfer. PMSG-based wind systems are often isolated from the grid during faults to prevent the damage of the fully rated back-to-back power converter and DC link capacitor [7, 8]. Grid code, however, mandates that a certain number of PMSGs be linked to the grid during fault events and thereby assist the grid. For PMSGs to support the PMSG-connected grid system by regulating real and reactive power and protecting the power electronic components in the system, appropriate fault ride-through (FRT) methods are required. Moreover, the application of optimization techniques or artificial intelligence-based controllers in wind side converters helps improve PMSG's performance [9, 10].

Robust and adaptive control systems must be used to deal with the nonlinearity of wind systems. Over the last two decades, meta-heuristic optimization techniques have become very popular. Length of the training procedure and convergence time are the shortcomings of artificial neural networks (ANNs) [11]. Although fuzzy logic control (FLC) is easy to build, cost-effective, and has better performance with the system's nonlinearities, it requires deep knowledge in design operation [12, 13]. There are several statistical and conventional techniques like the Taguchi technique, response surface method (RSM) [14], artificial neural network (ANN), and affine projection algorithm (APA) [15]. They are applied in fine-tuning proportional-integral

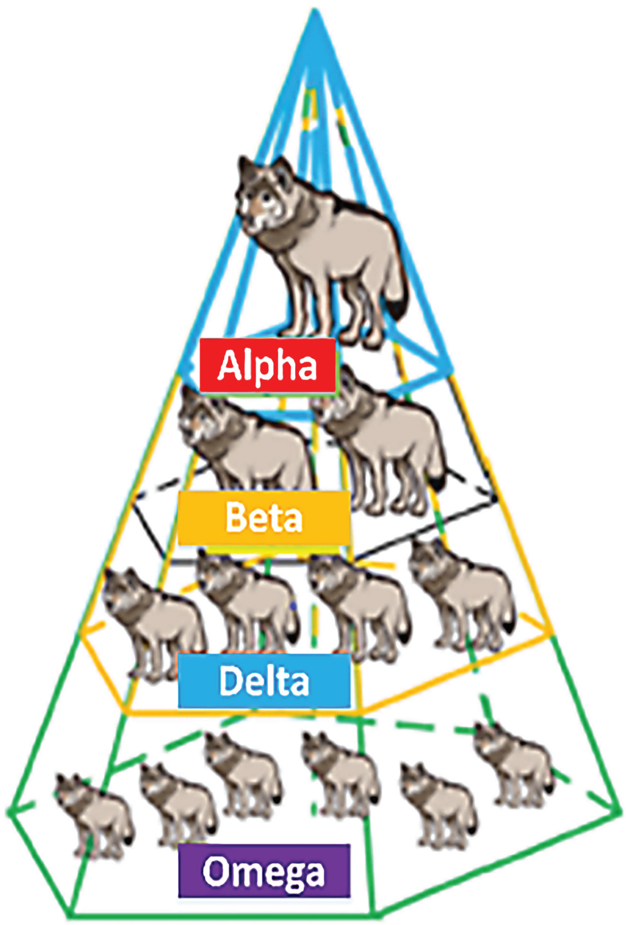

Fig. 2. Hierarchy of grey wolf (dominance decreases from the top down).

Fig. 3. Hunting actions of GWs [23].

(PI) controllers employed in the regulatory system of different power system components. These techniques, however, depend on the initial values. Thus, meta-heuristic algorithms such as particle swarm optimizer (PSO) [16], cuckoo search algorithm (CSA), whale optimizer algorithm (WOA) [17], bee algorithm (BA) [18], gravitational search algorithm (GSO), and differential evolution algorithm are competitive solutions for fine-tuning the parameters of PI controllers [15].

As the penetration of wind energy increases, the need to address FRT capability issues becomes more critical. Earlier, WTs were allowed to trip when a voltage dip occurred. During this voltage dip, active power provided to the grid by the WECS is instantaneously reduced. This power becomes at least temporarily lower than the mechanical power available at the rotor, hence, the rotor speed of the wind generator increases [19]. Controllable FRT capabilities used for PMSG wind systems, including pitch control system, modified converter system, and FLC-based GSC operation are discussed in [20]. In addition, there are many hardware solutions, like braking chopper system (BCS), FACTS, and energy storage devices (ESD) [7, 21].

This work investigates an OTC-MPPT strategy during wind speed change and FRT capability of PMSG wind system using BCS at the DC-bus in the course of faults with the support of optimized wind side controller based on GWO technique. The GWO efficacy is tested in a variety of situations. The paper structure is as follows: Section 2 focuses on the description of the system under consideration. A mathematical model of the GWO and its MSC application are considered in Sections 3 and 4, respectively. Simulation results are introduced and discussed in Section 5. Section 6 presents the conclusion.

II. Description of the studied system

Figure 1 depicts the overall structure of the system under investigation. It consists of a WT model; PMSG, MSC, and GSC with their control; and a grid model.

A. A WT model

The WT model can be defined as follows [7, 17]:

$$C_P\left(\lambda,\beta\right)=0.5176\left(\frac{116}{\lambda_i}-0.4\beta-5\right)\exp^{-\frac{21}{\lambda_i}}+0.0068\lambda\ ,$$

$$\lambda=\frac{\omega_r R}{V_W},$$

$$T_m=\frac{P_m}{\omega_r},$$

$$T_m=J_{eq}\frac{d\omega_r}{dt}+B_{eq}\omega_r+T_e\ ,$$

where C_P, λ, ω_r, J_{eq}, B_{eq}, T_e, T_m are the studied WT parameters [17].

B. A PMSG model

The PMSG concept is fully defined in [17] and can be represented as follows:

$$V_{ds}=R_s I_d+\dot{\lambda}_d-\omega_e\Psi_q\ ,$$

Initialize the grey wolf population X_i (i = 1, 2, ..., n)
Initialize a, A, and C
Calculate the fitness of each search agent
X_α=the best search agent
X_β=the second best search agent
X_δ=the third best search agent
***while** (t < Max number of iterations)*
    ***for** each search agent*
        Update the position of the current search agent by equation (3.7)
    end for
    Update a, A, and C
    Calculate the fitness of all search agents
    Update X_α, X_β, and X_δ
    t=t+1
end while
***return** X_α*

Fig. 4. Pseudo-code of the GWO algorithm [23].

$$V_{qs} = R_s I_q + \dot{\lambda}_q - \omega_e \psi_d \ .$$

The stator flux connection components can be written as:

$$\psi_d = L_d I_d + \psi_{pm},$$
$$\psi_q = L_q I_q.$$

The symbol T_e can be defined in the following way:

$$T_e = \frac{3}{2} n_p \left(\psi_d I_q - \psi_q I_d\right) = \frac{3}{2} n_p \left(\psi_{pm} I_q + I_d I_q \left(L_d - L_q\right)\right).$$

For the surface-mounted PMs sort, $L_q = L_d$. Then, T_e can be written as tracks:

$$T_e = \frac{3}{2} n_p \left(\psi_{pm} I_q\right).$$

III. A GWO approach

This study employs GWO to find the best controller settings. The four types of grey wolves (GWs) used to model the optimization technique's leadership structure are alpha (α), beta (β), delta (δ), and omega (ω) (Fig. 2). The hunters' choice is made by the leaders (α), as seen in Fig. 2. Wolves (β) assist in decision-making and also serve (α) as a wolf's counsel and the pack's enforcer. The (ω) wolves serve as scapegoats. This helps to keep the pack satisfied and the dominance structure in place. If a wolf is not a dominant α, β, or ω, it is described as subordinate [18]. The feeding behavior of GWs is seen in Fig. 3. In addition, the pseudo-code of the GWO algorithm is presented in Fig. 4.

The GWO mathematical formula seeks to mimic and recreate the numerous steps that GWs go through hunting prey, which are: social hierarchy (A), surrounding prey (B), hunting (C), attacking prey (D), and searching for prey (E).

The GWO concept is fully defined in [22] as follows:

$$\vec{D} = \left|\vec{c}\ \vec{x}_p(t) - \vec{x}(t)\right|,$$

$$\vec{x}(t+1) = \vec{x}_p(t) - \vec{A}\,\vec{D},$$

$$\vec{A} = 2\vec{a}\vec{r}_1 - \vec{a}\ ,$$

$$\vec{C} = 2\vec{r}_2\ \ ,$$

$$\vec{D}_\alpha = \left|\vec{C}_1\vec{x}_\alpha - \vec{x}\right|,\ \vec{D}_\beta = \left|\vec{C}_2\vec{x}_\beta - \vec{x}\right|,\ \vec{D}_\delta = \left|\vec{C}_3\vec{x}_\delta - \vec{x}\right|\ ,$$

$$\vec{X}_1 = \vec{x}_\alpha - \vec{A}_1\left(\vec{D}_\alpha\right),\ \vec{X}_2 = \vec{x}_\beta - \vec{A}_2\left(\vec{D}_\beta\right), \vec{X}_3 = \vec{x}_\delta - \vec{A}_3\left(\vec{D}_\delta\right),$$

$$\vec{x}(t+1) = \frac{\vec{X}_1 + \vec{X}_2 + \vec{X}_3}{3}\ .$$

IV. MSC control with GWO

As seen in Fig. 1, the job of MSC is to manage the machine rotor speed for maximizing output power from the passing wind, based on GWO. Equation (1) shows the system optimization model with control cost. Table 1 indicates the selection of PI-GWO controller gains employed at MSC for MPPT utilizing the OTC method. The PMSG control cost optimization model is as follows:

$$\begin{aligned} Minimize\ F(x) = \int_0^T & W_1\left|I_d - I_d^*\right| + W_2\left|\omega_m - \omega_m^*\right| + \\ & + W_3\left|I_q - I_q^*\right| + W_4\left|V_{dc} - V_{dc}^*\right| \end{aligned}, \quad (1)$$

where T is the average time, while 100 and 6 are the iterations' number and agents, respectively. W_1, W_2, W_3, and W_4 are used to compute the cost of control, which is 4×10^5 in our studied case.

V. The FRT capability enhancement method

Figure 5 depicts the grid coding necessities of some pioneer countries in the wind energy sector in the event of a failure [24, 25]. The graph indicates that, in an abnormal

Table 1. Gains of the PI controllers with GWO.

Technique	K_{p1}	K_{p2}	K_{i1}	K_{i2}
PI-GWO	2.932	2.932	199.2438	199.2438

Table 2. Indian grid code requirement.

Nominal grid voltage	Clearing time	V_{pf}	V_f
400 kV	100 ms	360 kV	60 kV
220 kV	160 ms	200 kV	33 kV
132 kV	160 ms	120 kV	19.8 kV
110 kV	160 ms	96.25 kV	16.5 kV
66 kV	300 ms	60 kV	9.9 kV

Table 3. BCS parameters.

Resistance value	1.5 Ω
Rated power	12 kW
Maximum temperature	150 °C
Thermal time constant	4 min
Weight	30 kg
Dimensions	(750.330.150) mm

Table 4. Parameters for simulated WECS [26].

Component	Parameter	Symbol	Value
WT	Blade radius	R	33.05 m
	Rated wind speed	v_W	12 m/s
	Optimal power coefficient	C_P	0.44
	Optimal tip speed ratio	λ_{opt}	10.5
	Wind density	ρ	1.225 kg/m^3
PMSG	Rated power	P	1.5 MW
	Rated stator voltage	V	575 V
	Pole pairs	p	40
	Generator stator resistance	R_s	0.01 pu
	Generator inductance in the *d* frame	L_d	0.7 pu
	Generator inductance in the *q* frame	L_q	0.7 pu
	Permanent magnet flux	ψ_{pm}	0.9 pu
BTB power converter	MSC frequency switching	$F_{sw\text{-}MSC}$	1 650 Hz
	GSC frequency switching	$F_{sw\text{-}GSC}$	1 650 Hz
	DC-Link voltage	V_{DC}	1 150 V
	DC-Link capacitor	C_{DC}	10 000 µF
	Grid frequency	F	60 Hz
LC Filter	Inverter side inductance	L_i	0.3 pu
	Inverter side resistance	R_i	0.003 pu
	Filter capacitor	C_f	0.0267 pu
	Damping resistance	R_d	0.003 pu

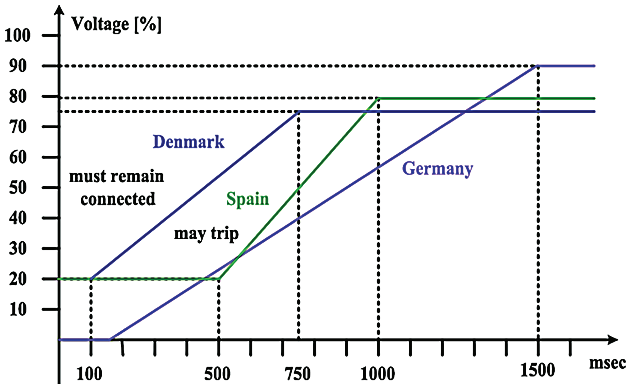

Fig. 5. FRT curve of grid code's pioneer nations in wind markets.

situation, the WT should be connected to the power grid for a known time according to each nation grid code, which fosters grid reliability. The fault clearing period, nominal system voltages, and fault clearing durations of the Indian grid code are all shown in Table 2. The V_f indicates that under a fault state, 15 percent of the nominal system voltage should be maintained, while the V_{pf} indicates the lowest voltage during normal wind system functioning. This paper investigates a simple cost-effective FRT capability enhancement method, namely a BCS, to get rid of surplus power at the DC bus and keep it in allowable ranges. Figure 6 shows a grid-connected PMSG including a BCS at the DC link. The used BCS parameters are listed in Table 3.

VI. Simulated results and discussion

MATLAB 2017b is used to evaluate the impact of the studied optimized controller on the performance of a grid-connected 1.5 MW PMSG-based wind system. The transient behaviors of the PMSG-based grid-connected system are investigated under symmetrical grid fault and step change of wind speed scenarios. The studied WECS parameters are listed in Table 4, and the used BCS parameters are given in Table 3.

Case 1: System performance as a result of step-change in wind speed.

In this case, PMSG with optimized controllers is tested under a step change of wind speed in the presence of an OTC technique to test the system's ability to realize MPPT.

A. WT performance

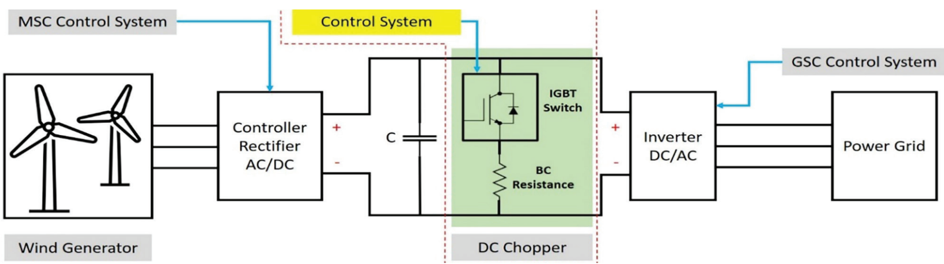

Fig. 6. BCS at the DC bus for grid-connected PMSG.

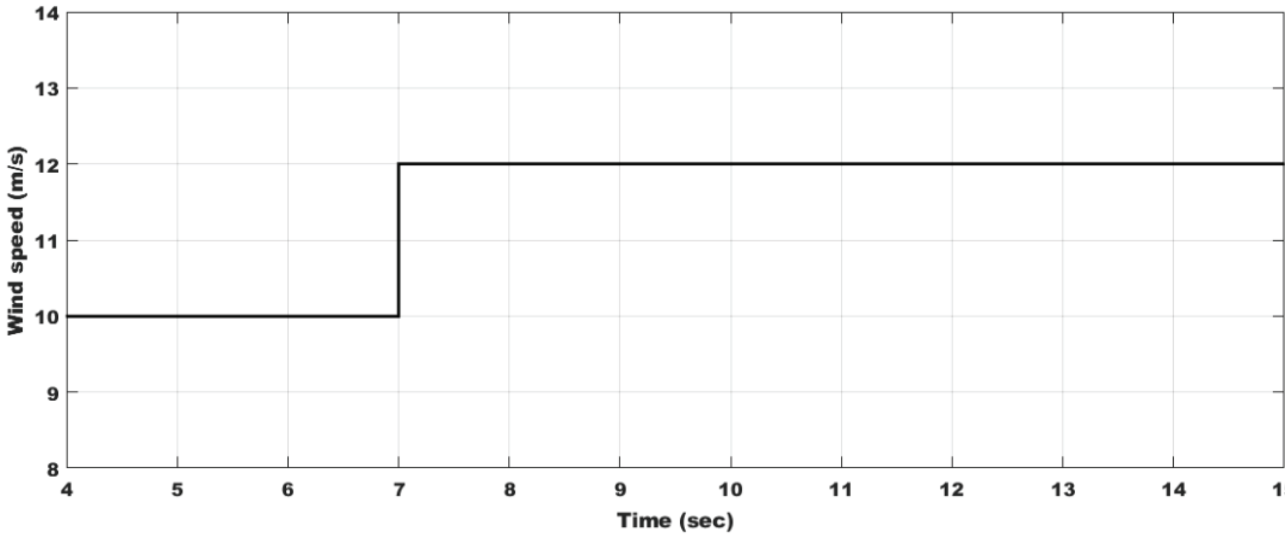

(a)

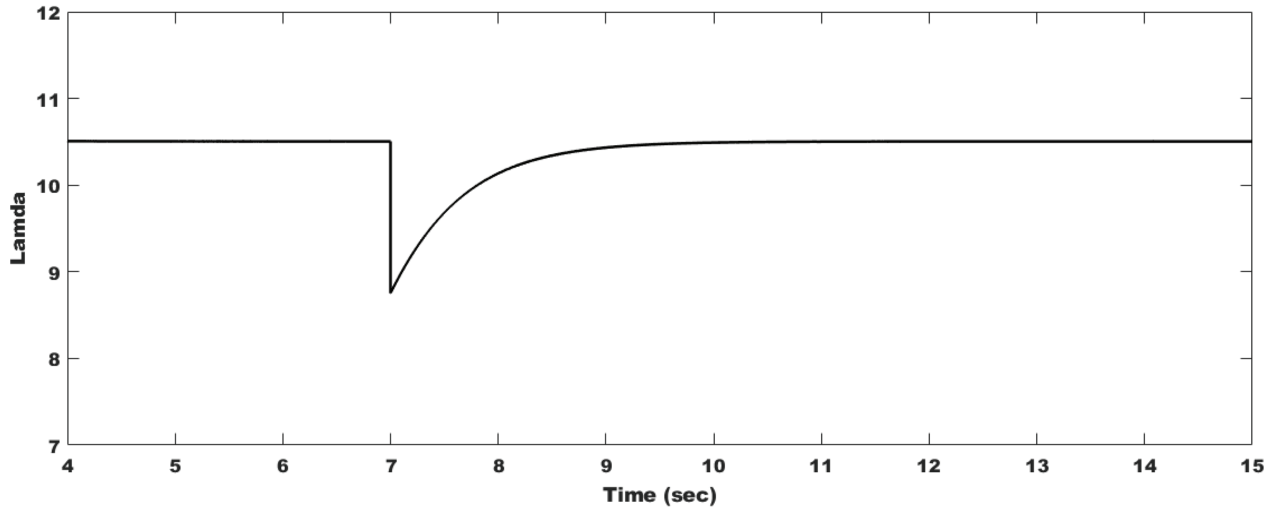

(b)

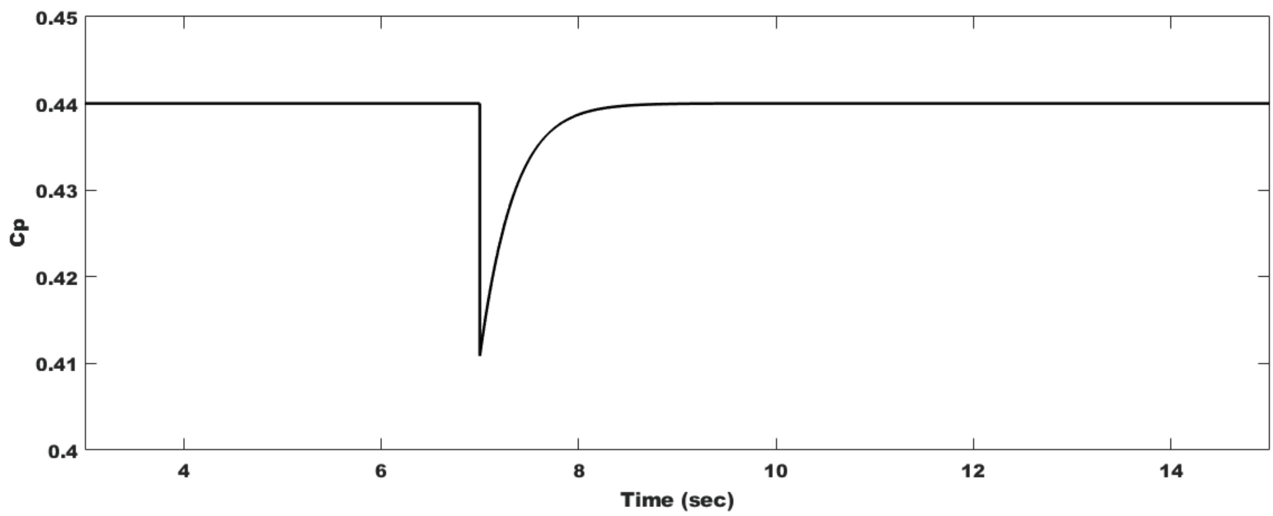

Fig. 7. WT performance: (a) wind speed profile, (b) λ, (c) C_P.

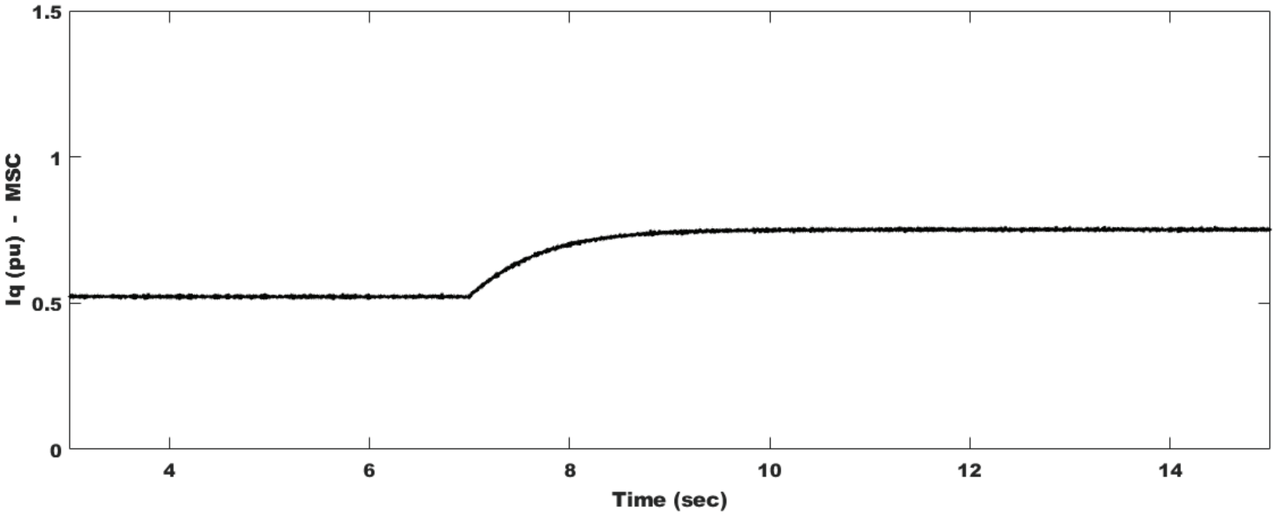

(a)

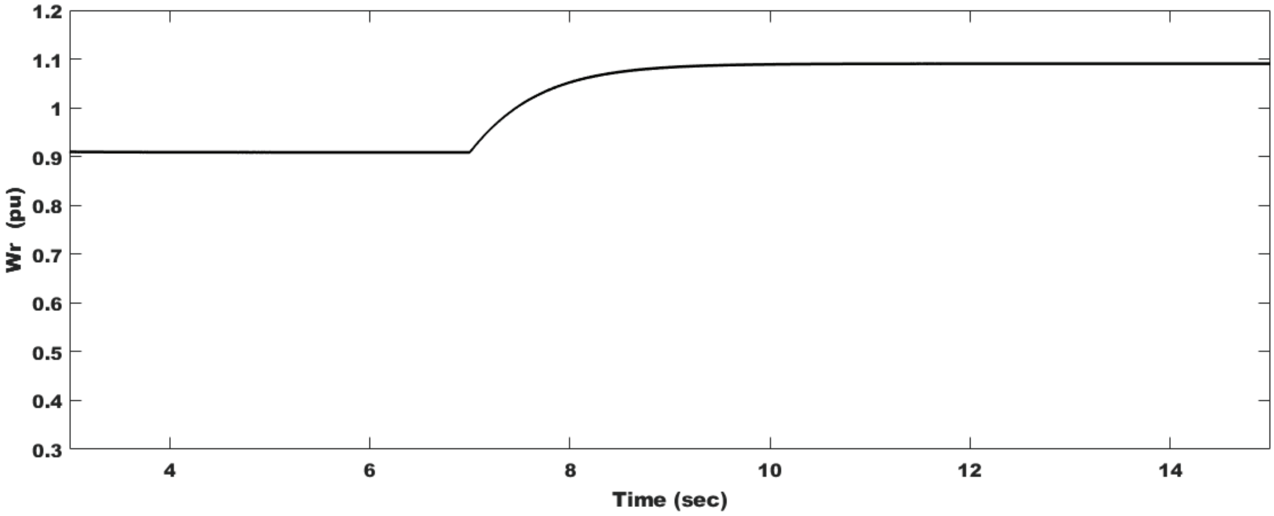

(b)

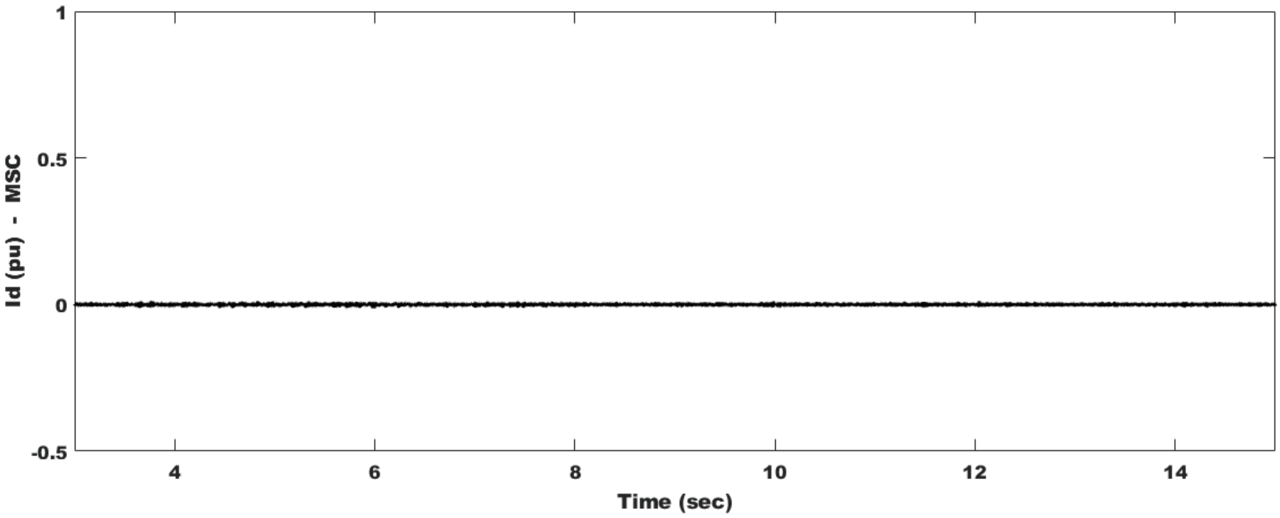

(c)

Fig. 8. MSC performance: (a) I_q-MSC, (b) ω_r, (c) I_d-MSC.

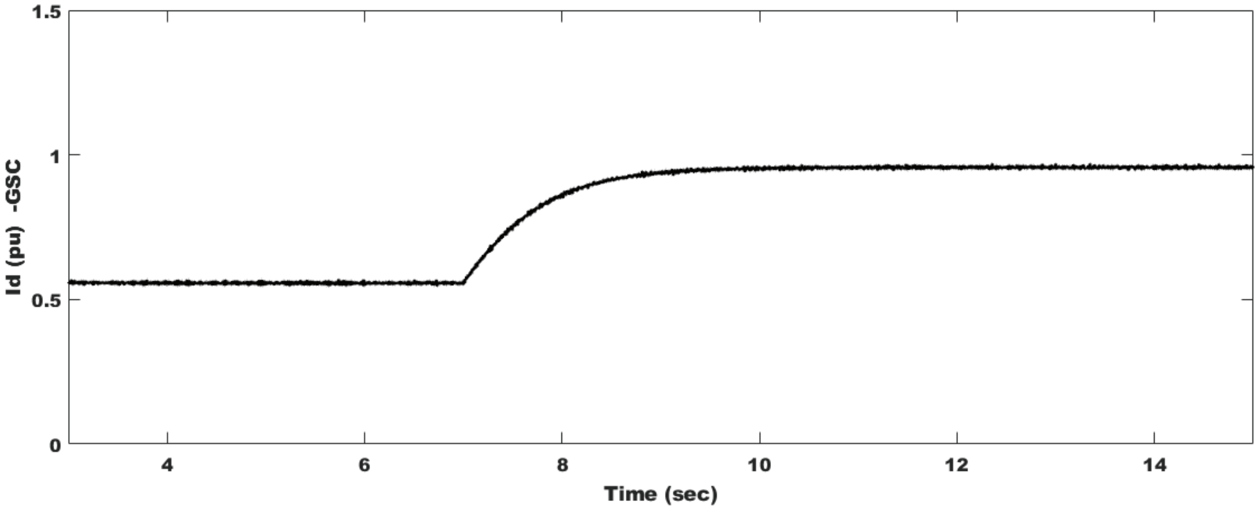

(a)

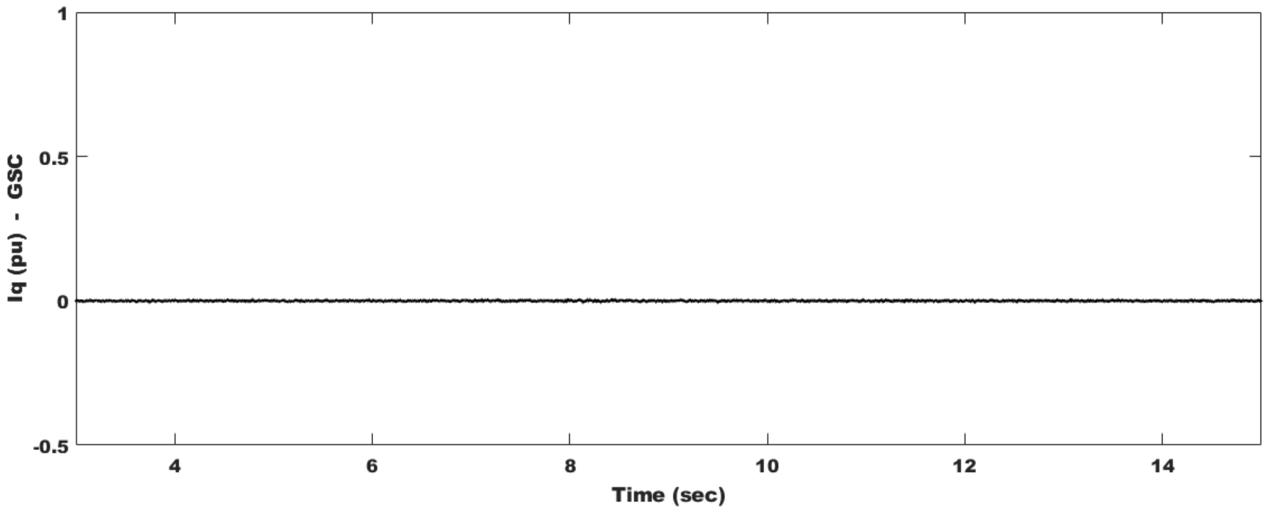

(b)

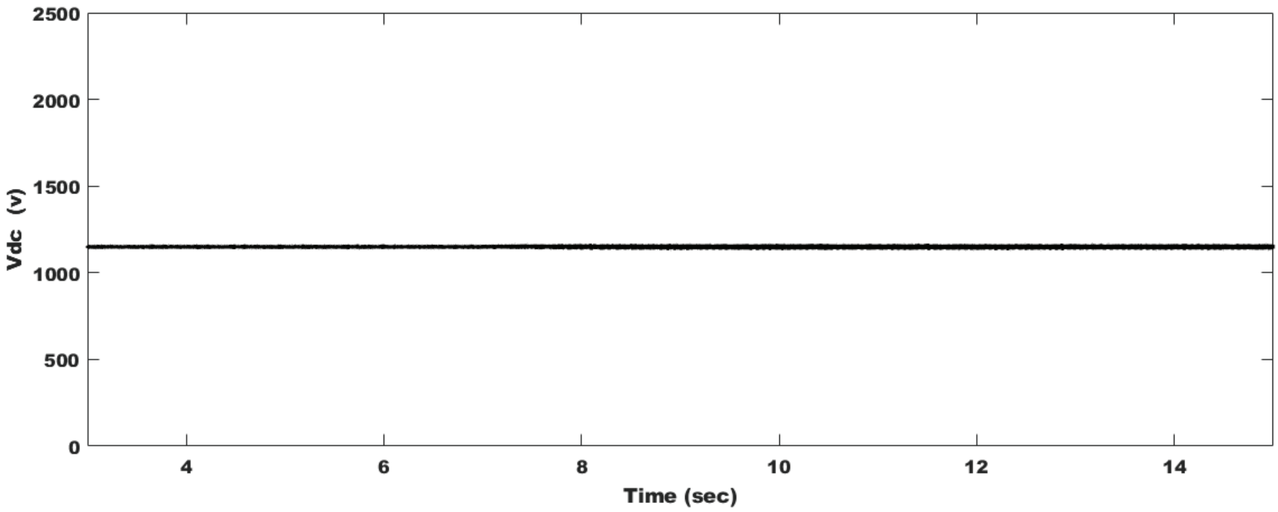

(c)

Fig. 9. GSC performance: (a) I_d-GSC, (b) I_q-GSC, (c) V_{DC}.

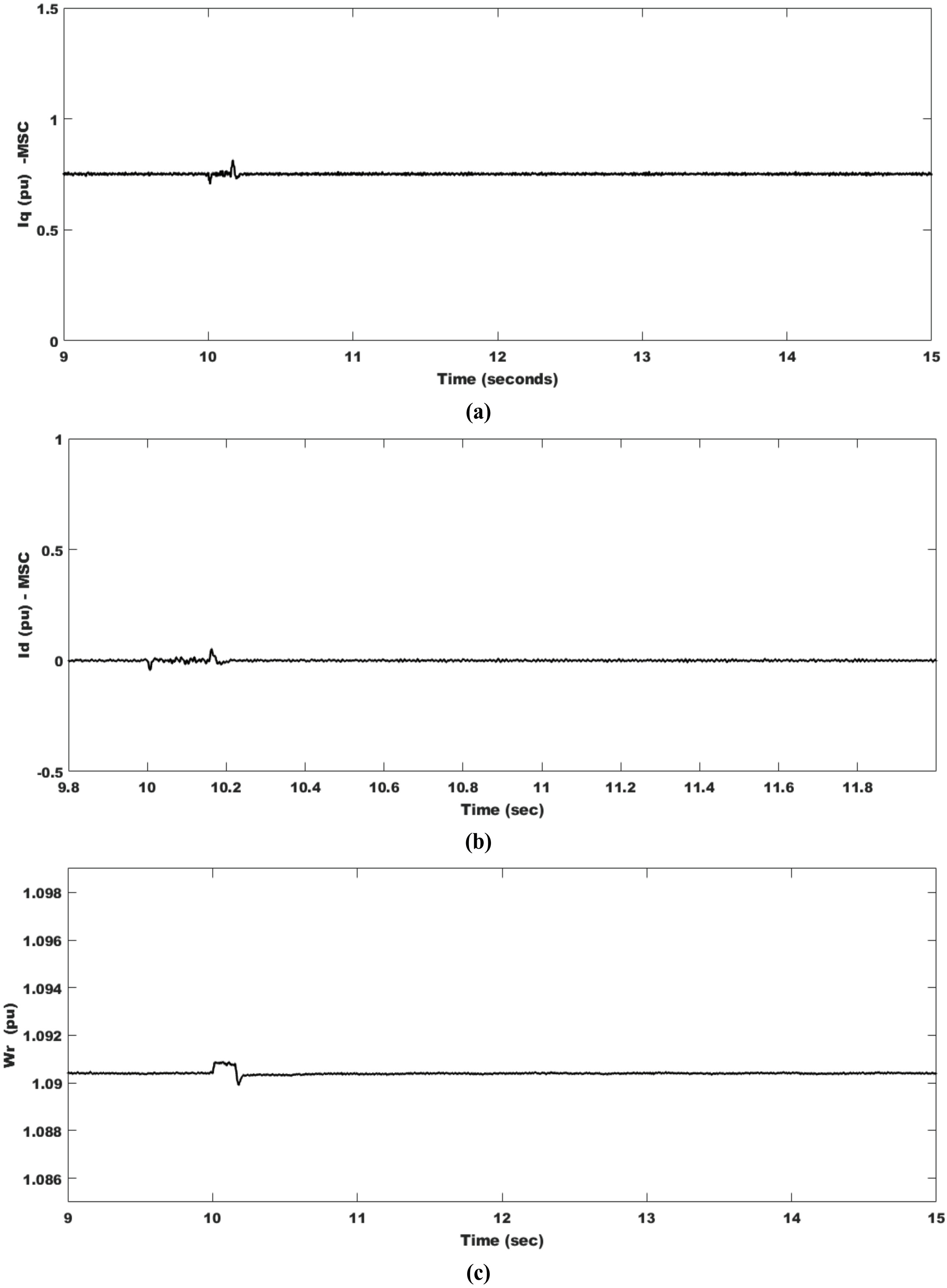

Fig. 10. MSC performance: (a) I_q-MSC, (b) I_d-MSC, (c) ω_r.

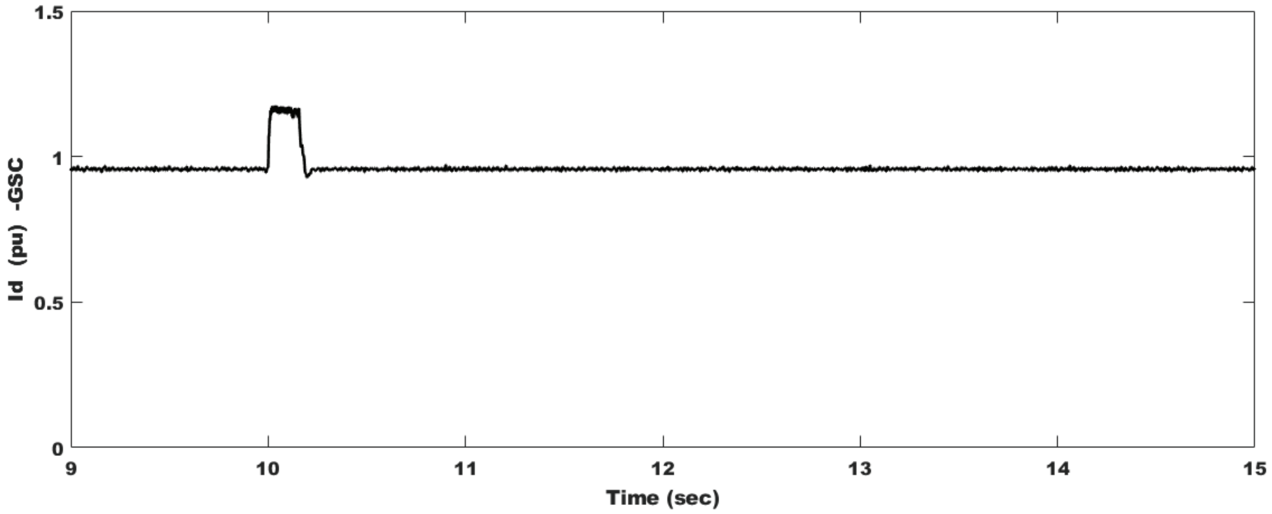

(a)

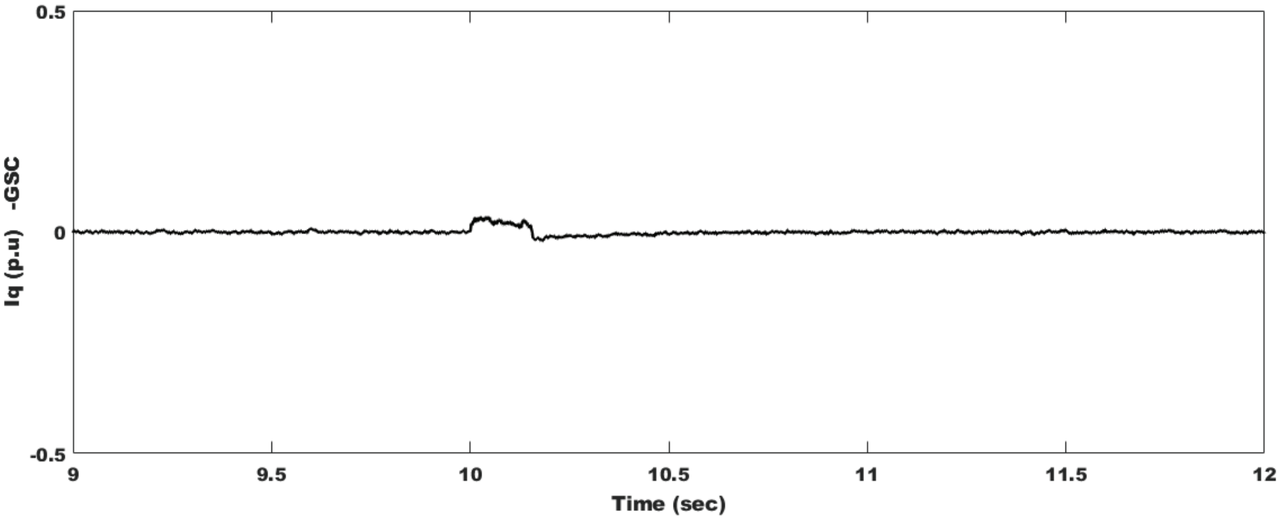

(b)

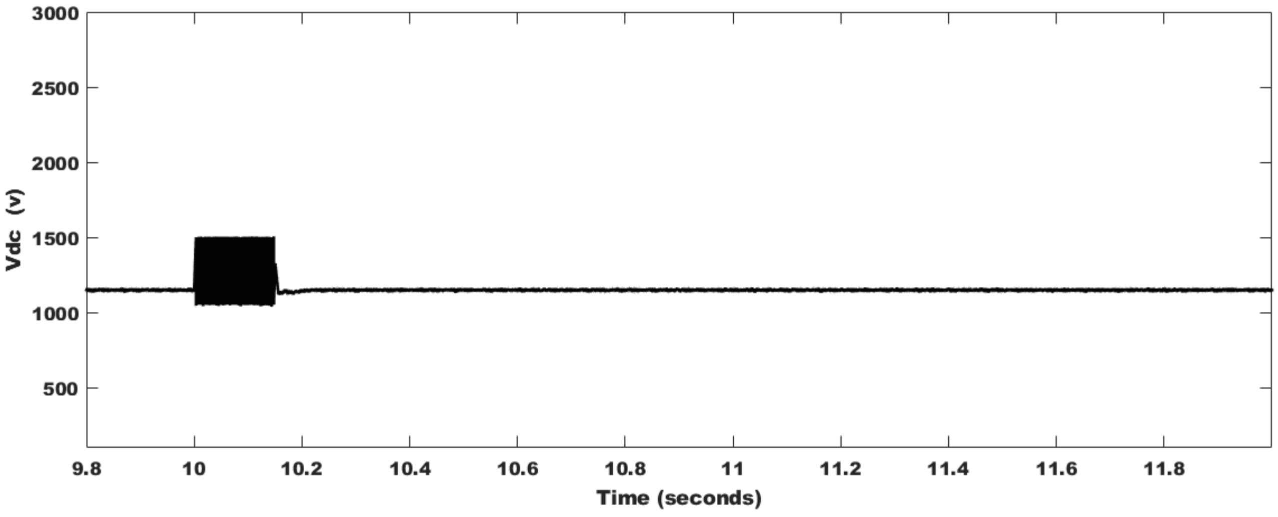

(c)

Fig. 11. GSC performance: (a) I_d-GSC, (b) I_q-GSC, (c) V_{DC}.

Figure 7 shows the WT characteristics. A step change in the wind speed, with an average speed of 11 m/s, is studied to assess the proposed controller (Fig. 7(a)). Both λ and C_P, which ensure operation at optimal values (10.5 and 0.44), are presented in Figures 7(b) and 7(c). With the optimized controller, the system reaches the optimal values rapidly, in 0.987 seconds roughly.

B. MSC performance

Figures 8(a) and 8(b) demonstrate that when the wind speed increases the MSC quadrature current and electrical angular speed rise. With the optimized controller, the system tracks the reference values rapidly, in 1.427 seconds roughly. Figure 8(c) shows that the MSC direct current is set to zero for maximal torque production and high efficiency.

C. GSC performance

Figure 9(a) demonstrates that GSC direct current rises when the wind speed increases. With the optimized controller, the system tracks the reference values rapidly, in 1.847 seconds roughly. The GSC quadrature current (Fig. 9(b)) is zero due to the unity power factor operation. Figure 9(c) shows that the V_{DC} is maintained constant because of the GSC controller's capabilities, which indicates that all the generated power is transferred from MSC to GSC.

Case 2: System performance as a result of a 3-phase fault.

In this case, PMSG with optimized controllers is subjected to a three-phase fault in the presence of a BCS to test the system's ability to realize FRT.

A. MSC performance

As seen in Figure 10, combining the GWO and BCS during the fault time suppresses transient oscillations in the system parameters, thereby increasing the PMSG's FRT capability. Figures 10(a) and 10(b) show small oscillations in MSC quadrature current and MSC direct current, respectively. These oscillations are below 2%, which reflects the role of the optimized controller. Figure 10(c) shows an increase in ω due to the voltage dip, where the system tries to supply the fault.

B. GSC performance

Figures 11(a) and 11(b) show GSC direct current and GSC quadrature current increase during the dip in grid voltage to maintain constant injected active power. These Figures also indicate very few oscillations in I_d and I_q of GSC. The reactive current rises during the fault to support the grid voltage (Fig. 11(b)). Figure 11(c) points out a small overvoltage in V_{DC} (a 30.4 % over-voltage during the fault period), and the system reaches its steady-state value (1150 V) after the fault is cleared.

VII. Conclusion

In this study, the dynamic performance of the PMSG-based WT system is enhanced by using the GWO approach. The clear benefits of the suggested technique (optimized MSC controllers) are efficient MPPT extraction, FRT capability improvement, decreased overshoot/undershoot performance, and smooth steady-state performance. The power and control circuits in MATLAB are used to implement the mathematical model of the addressed system. The response of PMSG's parameters is presented for two scenarios (a step change in wind speed and three-phase fault) to assess the robustness of the GWO technique and findings suggest that it was successful in achieving the FRT and MPPT objectives. The performance of WT, MSC, and GSC is studied during the wind speed changes and the investigated fault, and the parameters are shown to track their reference values rapidly. In the end, it can be stated that a GWO-based PI controller used at MSC enables greater PMSG penetration in modern power systems.

Conflict of interest:

The authors declare that they have no conflict of interest.

References

[1] REN21, *Renewables 2020 Global Status Report*. 2020.

[2] M. K. Ratib and A. Rashwan, "Amplitude Sampled Reference-Based Space Vector Pulse Width Modulation for Control of Voltage Source Converters," *Energy Syst. Res.*, vol. 4, no. 2, pp. 46–63, 2021.

[3] N. Sekhar and N. Kumaresan, "Operation and control of a stand-alone power system with integrated multiple renewable energy sources," *Wind Eng.*, 2021, DOI: 10.1177/0309524X211024126.

[4] M. M. Mahmoud, M. Khalid Ratib, M. M. Aly, and A. M. M. Abdel-Rahim, "Wind-driven permanent magnet synchronous generators connected to a power grid: Existing perspective and future aspects," *Wind Eng.*, 2021, DOI: 10.1177/0309524X211022728.

[5] M. M. Mahmoud, M. M. Aly, H. S. Salama, and A. M. M. Abdel-Rahim, "Dynamic evaluation of optimization techniques–based proportional-integral controller for wind-driven permanent magnet synchronous generator," *Wind Eng.*, vol. 45, no. 3, pp. 696–709, 2021, DOI: 10.1177/0309524X20930421.

[6] M. M. Mahmoud, A. Mohamed Hemeida, and A. M. M. Abdel-Rahim, "Behavior of PMSG Wind Turbines with Active Crowbar Protection under Faults," in *2019 Innovations in Power and Advanced Computing Technologies, i-PACT 2019*, 2019, pp. 1–6, DOI: 10.1109/i-PACT44901.2019.8960004.

[7] M. M. Mahmoud, A. M. Hemeida, T. Senjy, and A. M. Ewais, "Fault Ride-Through Capability Enhancement for Grid-Connected Permanent Magnet Synchronous Generator Driven by Wind Turbines," in *IEEE Conference on Power Electronics and Renewable Energy, CPERE 2019*, 2019, pp. 567–572, DOI: 10.1109/CPERE45374.2019.8980139.

[8] M. M. Mahmoud, M. M. Aly, H. S. Salama, and A.-M. M. Abdel-Rahim, "An internal parallel capacitor

control strategy for DC-link voltage stabilization of PMSG-based wind turbine under various fault conditions," *Wind Eng.*, p. 0309524X2110606, 2021, DOI: 10.1177/0309524x211060684.

[9] K. Tazi, M. F. Abbou, and F. Abdi, "Performance analysis of micro-grid designs with local PMSG wind turbines," *Energy Syst.*, vol. 11, no. 3, pp. 607–639, 2020, DOI: 10.1007/s12667-019-00334-2.

[10] M. M. Mahmoud, M. K. Ratib, M. M. Aly, A. Moamen, and M. A. Rahim, "Effect of Grid Faults on Dominant Wind Generators for Electric Power System Integration : A Comparison and Assessment," *Energy Syst. Res.*, vol. 4, no. 3, pp. 70–78, 2021.

[11] S. K. Arumugasamy, Z. Y. Chen, L. D. Van Khoa, and H. Pakalapati, "Comparison between Artificial Neural Networks and Support Vector Machine Modeling for Polycaprolactone Synthesis via Enzyme-Catalyzed Polymerization," *Process Integr. Optim. Sustain.*, vol. 5, no. 3, pp. 599–607, 2021, DOI: 10.1007/s41660-021-00163-w.

[12] M. M. Mahmoud, M. M. Aly, H. S. Salama, and A. M. M. Abdel-Rahim, "A combination of an OTC based MPPT and fuzzy logic current control for a wind-driven PMSG under variability of wind speed," *Energy Syst.*, no. 0123456789, 2021, DOI: 10.1007/s12667-021-00468-2.

[13] K. Anil Naik, "Real-time implementation of interval type-2 fuzzy logic based damping controller for wind integrated power system," *Wind Eng.*, 2021, DOI: 10.1177/0309524X211030186.

[14] M. N. Uddin and I. K. Amin, "Adaptive Step Size Based Hill-Climb Search Algorithm for MPPT Control of DFIG-WECS With Reduced Power Fluctuation and Improved Tracking Performance," *Electr. Power Components Syst.*, vol. 46, no. 19–20, pp. 2203–2214, Dec. 2018, DOI: 10.1080/15325008.2018.1533603.

[15] M. H. Qais, H. M. Hasanien, S. Alghuwainem, and M. A. Elgendy, "Output Power Smoothing of Grid-Tied PMSG-Based Variable Speed Wind Turbine Using Optimal Controlled SMES," 2019, DOI: 10.1109/UPEC.2019.8893530.

[16] S. Phommixay, M. L. Doumbia, and Q. Cui, "Comparative Analysis of Continuous and Hybrid Binary-Continuous Particle Swarm Optimization for Optimal Economic Operation of a Microgrid," *Process Integr. Optim. Sustain.*, 2021, DOI: 10.1007/s41660-021-00193-4.

[17] M. M. Mahmoud, M. M. Aly, and A. M. M. Abdel-Rahim, "Enhancing the dynamic performance of a wind-driven PMSG implementing different optimization techniques," *SN Appl. Sci.*, vol. 2, no. 4, 2020, DOI: 10.1007/s42452-020-2439-3.

[18] M. H. Nadimi-Shahraki, S. Taghian, and S. Mirjalili, "An improved grey wolf optimizer for solving engineering problems," *Expert Syst. Appl.*, vol. 166, 2021, DOI: 10.1016/j.eswa.2020.113917.

[19] C. Kim and W. Kim, "Enhanced Low-Voltage Ride-Through Coordinated Control for PMSG Wind Turbines and Energy Storage Systems Considering Pitch and Inertia Response," *IEEE Access*, vol. 8, pp. 212557–212567, 2020, DOI: 10.1109/ACCESS.2020.3040905.

[20] M. Metwally Mahmoud, H. S. Salama, M. M. Aly, and A. M. M. Abdel-Rahim, "Design and implementation of FLC system for fault ride-through capability enhancement in PMSG-wind systems," *Wind Eng.*, 2020, DOI: 10.1177/0309524X20981773.

[21] M. Nasiri, J. Milimonfared, and S. H. Fathi, "A review of low-voltage ride-through enhancement methods for permanent magnet synchronous generator-based wind turbines," *Renewable and Sustainable Energy Reviews*, vol. 47. pp. 399–415, 2015, DOI: 10.1016/j.rser.2015.03.079.

[22] S. Mirjalili, S. M. Mirjalili, and A. Lewis, "Grey Wolf Optimizer," *Adv. Eng. Softw.*, vol. 69, pp. 46–61, 2014, DOI: 10.1016/j.advengsoft.2013.12.007.

[23] C. Muro, R. Escobedo, L. Spector, and R. P. Coppinger, "Wolf-pack (Canis lupus) hunting strategies emerge from simple rules in computational simulations," *Behav. Processes*, vol. 88, no. 3, pp. 192–197, 2011, DOI: 10.1016/j.beproc.2011.09.006.

[24] A. Rini Ann Jerin, P. Kaliannan, and U. Subramaniam, "Improved fault ride-through capability of DFIG based wind turbines using synchronous reference frame control based dynamic voltage restorer," *ISA Trans.*, vol. 70, pp. 465–474, 2017, DOI: 10.1016/j.isatra.2017.06.029.

[25] M. Nasiri and A. Arzani, "Robust control scheme for the braking chopper of PMSG-based wind turbines–A comparative assessment," *Int. J. Electr. Power Energy Syst.*, vol. 134, 2022, DOI: 10.1016/j.ijepes.2021.107322.

[26] H. Geng, G. Yang, D. Xu, and B. Wu, "Unified power control for PMSG-based WECS operating under different grid conditions," *IEEE Trans. Energy Convers.*, vol. 26, no. 3, pp. 822–830, 2011, DOI: 10.1109/TEC.2011.2127478.

Mohamed Metwally Mahmoud was born in Sohag, Egypt, in 1992. He received the B.Sc. and M.Sc. degrees in Electrical Engineering from Aswan University, Aswan, Egypt, in 2015 and 2019, respectively. Since 2017, he has been with the Department of Electrical Engineering, Aswan University, as a Teaching Assistant. His research interests include performance improvement of wind generators, optimization methods, FLC method, fault ride-through capability, and energy storage systems.

Mohamed Khalid Ratib was born in Sohag, Egypt, in 1993. He received the B.Sc. and M.Sc. degrees in Electrical Engineering from Aswan University, Aswan, Egypt, in 2016 and 2020, respectively. Since 2017, he has been with the Department of Electrical Engineering, Aswan University, as a Teaching Assistant. His research interests include power converters, MPC technique, PWM techniques.

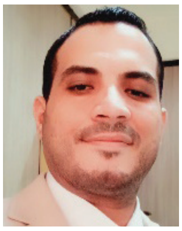

Abdallah E. Elwakeel was born in Karf El-Shika, Egypt, in 1989. He received the B.Sc. and M.Sc. degrees in Agricultural Engineering from Alexandria University, Alexandria, Egypt, in 2012 and 2017, respectively; and received the Ph.D. in Agricultural Engineering from Aswan University, Aswan, Egypt, in 2021. His research interests include electrical machines and farm machinery.

Basiony Shehata Atia was born in Kafr Elshiekh, Egypt, in 1996. He received a B.Sc. degree in Electrical Engineering from Aswan University, Aswan, Egypt, in 2019. Currently, he is a Field Service Engineer at BPI Department for Rapiscan Service Center Egypt, American Science and Engineering, Inc. Cairo, Egypt. His research interests include the performance improvement of renewable energy systems.

Mohamed M. Aly was born in Qena, Egypt, in 1974. He received a B.Sc. degree in Electrical Engineering from Assuit University, Assuit, Egypt, in 1995. He received both M.Sc. and Ph.D. from the UK. Now, he is a full professor at the Department of Electrical Engineering, Aswan University. His research interests include renewable energy systems, fault current limiters, and energy storage systems.

Abdel-Moamen M. Abdel-Rahim was born in Qena, Egypt, in 1971. He received the B.Sc. and M.Sc. degrees in Electrical Engineering from Assuit University, Assuit, Egypt, in 1992 and 1997, respectively. Since 1994, he has been with the Department of Electrical Engineering, Aswan University, as a Teaching Assistant. His research interests include optimal power flow and FACTS tools.